LLNL-JRNL-403585

LAWRENCE LIVERMORE NATIONAL LABORATORY

Time-Resolved X-Ray and Extreme Ultraviolet Spectrometer for Use on the National Spherical Torus Experiment

P. Beiersdorfer, J. K. Lepson, M. Bitter, K. W. Hill, L. Roquemore

May 7, 2008

Review of Scientific Instruments

Time-Resolved X-Ray and Extreme Ultraviolet Spectrometer for Use on the National Spherical Torus Experiment

P. Beiersdorfer[1], J. K. Lepson[2], M. Bitter[3], K. W. Hill[3], L. Roquemore[3]

[1] *Lawrence Livermore National Laboratory, Livermore, CA 94550, USA*

[2] *University of California, Berkeley, CA 94720, USA*

[3] *Princeton Plasma Physics Laboratory, Princeton, NJ 08543, USA*

Abstract

We describe upgrades to a compact grazing-incidence spectrometer utilized on the National Spherical Torus Experiment (NSTX) for monitoring light and heavy impurities . A fast-readout charge couple device (CCD) camera has been implemented that allows the recording of spectra with up to 25 ms time integration. This capability is used to study the time evolution of the K-shell emission of hydrogenlike and heliumlike boron, carbon, nitrogen, and oxygen between 10 and 65 Å. Different camera positioning pieces have been employed to extend the possible spectral range to as high as 140 . Several lines that cannot be ascribed to the usual elements found in the plasma have been observed in this spectral range, though often only in a few isolated discharges.

I. INTRODUCTION

The soft x-ray and extreme ultraviolet spectral region between 10 and 100 Å contains both the K-shell emission of the light elements B, C, N, and O as well as the L-shell emission of heavier elements, such as Ar, Ti, Fe, and Ni. This makes high-resolution observations of this spectral region very important for monitoring the relative concentration of these elements.

Recently, we have implemented a spectrometer, dubbed XEUS, on the NSTX magnetic fusion facility at Princeton to record the x-ray and extreme ultraviolet region with high-resolution [1]. The resolution achieved was about 0.1 Å, which was more than sufficient to resolve the K-shell emission from hydrogenlike and heliumlike ions in this region. The spectral range extended from about 10 Å to 65 Å. Time resolution was achieved by use of a shutter, which could open and close in about 30 ms, which allowed recording of a single spectrum from a given discharge. Here we report on several modifications to the instrument, which allow us to record multiple, time-resolved spectra. The new capability has enabled us to measure the variation of the relative impurity concentrations and thus to determine possible sources of various elements entering the plasma. We have also implemented a new camera mounting piece that extends the spectral range to as high as 140 Å.

II. SPECTROMETER DESIGN AND RECENT MODIFICATIONS

The XEUS diagnostic is among several instruments that have been developed at the Livermore electron beam ion trap facility and are now implemented on magnetic fusion devices [2,3]. XEUS employs a variable line spacing grating with an average line spacing of 2400 ℓ/mm [4] that produces a flat-field image at a focal distance of about 23 cm [1]. It is located at the end of the NSTX pump duct, which is about ten meters away from the vacuum vessel, and no shielding is employed against either hard x rays or neutrons. Its line of sight follows a radial line to the center stack of the tokamak within the horizontal midplane of the plasma.

A. Time response

When the instrument was first placed on NSTX, spectra were recorded with a Photometrics charge couple device (CCD) camera [1]. We have replaced this camera with a Princeton Instruments CCD PI-SX:1300/VON camera with a back-illuminated detector chip of similar, $1'' \times 1''$ size. The pixel width in this camera is 20 μm, which is 20% smaller than before. As before, the camera is liquid nitrogen cooled and operates at -110^o C.

Using the slow (50 kHz) readout mode, a full-size spectral image with 1340 by 1300 pixels is transfered from the camera to the hard drive in a little over half a minute. This time is cut considerably by using the fast (1 MHz) readout mode. But readout is still over one second, which is more than the < 1 s NSTX discharge duration. An additional increase in readout speed is accomplished by binning along the spectral and non-spectral axes. Readout times below 25 ms were achieved by reducing the camera image to 670 by 1 pixels and using the fastest computer available to us. Collapsing the 1300 vertical pixels to one, however, comes at an unacceptable expense, as we discuss in the following. Instead, we binned our spectra by a factor of 130 along the non-spectral axis and not at all along the spectral axis. In other words, we set the detector software to read out images of 1340 by 10 pixels . The readout time was about 90 ms per image and limited by the speed of our Dell computer. A typical sequence of eight such images recorded during the course of a NSTX discharge is shown in Fig. 1.

The camera is sensitive to hard x rays and cosmic rays. In principle, such events can be filtered out by setting an upper threshold when 1340 by 1300 pixels are available. Binning along the vertical axis, which has to be done *before* a pulse hight analysis is made, means that information on hard x-ray events is lost. Our choice of binning the vertical pixels by 130 gives us, in principle, ten independent spectra and allows us to test for the reproducibility of the line intensities, which in turn allows us to rule out the strongest hard x-ray events.

It is also very difficult to perfectly align the camera so that one readout axis is parallel to the spectroscopic axis and the other is perpendicular. In reality, there is a slant of a few pixels. In addition, a given spectral line is not perfectly straight but slightly curved. Binning along the vertical axis thus broadens a given line. For example, a line, which is typically 3 pixels wide and slanted by 6 pixels over the 1300 pixel vertical axis, will have a width that is almost three times as wide when binned along the vertical axis. We chose a binning factor of 130 because this still allows us to correct for (minor) misalignments of the spectral lines with the vertical axis.

The spectral resolution also suffers by using the fast, 1 MHz readout. At this speed, charge bleeds along the readout direction, which in our case is aligned with the spectral axis. This broadens the line. Moreover, because not as much charge is collected in the peak of the line, the signal to noise ratio suffers as well. The spectral resolution is illustrated in Fig. 2, where we show a spectral lineout from frame 7 of the eight images shown in Fig. 1. The line width is about twice of what it is when the 50 kHz readout is employed, i.e., the resolution is reduced by half. The bleeding increases with the intensity of the line, and the highest intensity lines we observed were broadened by as much a 0.35 Å, which is more than three times broader than in the slow readout mode.

The current readout speed was sufficient to measure the time variation of the K-shell line emission of highly charged boron, carbon, nitrogen, and oxygen ions. This is illustrated in Fig. 3(a). The data show that during this disharge the amount of nitrogen and boron increases during the course of the discharge relative to that of carbon, as illustrated in Fig. 3(b). Because boron nitride is used as shielding material of the radio frequency (RF) antennae, this increase indicates that an erosion of such material takes places during neutral-beam heating. Molybdenum and titanium shielded by the boron nitride may be exposed and also sputter into the disharge. In a few discharges, we have seen an indication that this may indeed happen, as illustrated by the spectrum from shot 123721 shown in Fig. 4. This spectrum contains a few lines that are otherwise not seen in NSTX discharges. These lines are tentatively ascribed to emission from neonlike Ti^{12+} and argonlike and chlorinelike Mo^{24+} and Mo^{25+} ions.

In principle, there is enough flux to record the line emission with even faster time resolution. The spectrum in Fig. 2, which was taken toward the end of the discharge when the emission is already reduced, still has an excellent signal to noise ratio for even the weaker lines. A factor of ten higher time solution is thus readily possible. During the main part of the discharge, when 4 MW of neutral beam power and 4 MW of RF wave heating were applied, even faster time resolution could in principle be achieved. In fact, the intensity of the N VII Lyman-α line is at least 50 times stronger in frame 4 than in frame 7, as illustrated in Fig. 3(a). The signal level thus would be sufficient to attain a time resolution of 0.2 ms or better. We have not achieved this kind of readout speed with the present setup. However, the present data show that this will be possible in the future with the current spectrometer, if a detector with yet faster readout and similar quantum efficiency ($\geq$ 20 %) was employed.

B. Extended wavelength coverage

The grating used in the present spectrometer affords flat-field imaging for wavelengths in excess of 100 Å [4]. To take advantage of this feature we have implemented a new mounting piece for the CCD camera to record spectra with longer wavelength. A typical spectrum is given in Fig. 5. The spectrum shows a multitude of iron lines near 100 Å, which are of interest to astrophysics and as tokamak diagnostics [5–7]. Spectral resolution of 0.1 Å was achieved, which is similar to that achieved at the short wavelengths.

Test measurements were made to cover the wavelength region as high as 140 Å. This is the region that contains the K-shell emission of hydroglike lithium, which is of great interest for lithium-injection experiments. These tests were successful. However, because of the finite extend of the CCD chip, this comes at losing coverage of the K-shell emission of B, C, N, and O between 15 and 65 Å. The longer wavelength region will thus be covered in the future by a second instrument, dubbed XEUS-II. It was also developed on the Livermore electron beam ion traps [8], and has been in use on the SSPX spheromak until its shutdown in fall of 2007 [3,9].

ACKNOWLEDGMENTS

This work was performed under the auspices of the US DOE by LLNL under contracts W-7405-ENG-48 and DE-AC52-07NA-27344 and supported by the Office of Fusion Energy Basic and Applied Plasma Science Initiative.

This work performed under the auspices of the U.S. Department of Energy by Lawrence Livermore National Laboratory under Contract DE-AC52-07NA27344.

REFERENCES

[1] P. Beiersdorfer, M. Bitter, L. Roquemore, J. K. Lepson, and M.-F. Gu, Rev. Sci. Instrum. **77**, 10F306 (2006).

[2] P. Beiersdorfer, Can. J. Phys. **86**, 1 (2008).

[3] A. T. Graf, S. Brockington, R. Horton, S. Howard, P. B. D. Hwang, J. Clementson, D. Hill, M. May, H. Mclean, R. Wood, M. Bitter, J. Terry, W. L. Rowan, J. K. Lepson, and L. Delgado-Aparicio, Can. J. Phys. **86**, 307 (2008).

[4] N. Nakano, H. Kuroda, T. Kita, and T. Harada, Appl. Optics **23**, 2386 (1984).

[5] P. Beiersdorfer, Ann. Rev. Astron. Astrophys. **41**, 343 (2003).

[6] J. Lepson, P. Beiersdorfer, M. Bitter, and S. M. Kahn, Can. J. Phys. **86**, 175 (2008).

[7] B. C. Stratton, H. W. Moos, and M. Finkenthal, Astrophys. J. **279**, L31 (1984).

[8] P. Beiersdorfer, J. R. Crespo López-Urrutia, P. Springer, S. B. Utter, and K. L. Wong, Rev. Sci. Instrum. **70**, 276 (1999).

[9] J. Clementson, P. Beiersdorfer, M. F. Gu, H. S. McLean, and R. D. Wood, J. Phys. Conf. Ser. in press (2008).

FIGURES

FIG. 1. Sequence of 1340 by 10 pixel spectral images obtained with XEUS for NSTX shot 123629. The locations of the dominant K-shell lines of boron, carbon, nitrogen, and oxygen are marked.

FIG. 2. K-shell emission features observed with XEUS in frame 7 during NSTX shot 123629. Lines are labeled by the emitting ion. Ly-α denotes the $2p \rightarrow 1s$ transition in hydrogenlike ions; w and y denote the $1s2p\ ^1P_1 \rightarrow 1s^2\ ^1S_1$ resonance and the $1s2p\ ^3P_1 \rightarrow 1s^2\ ^1S_1$ intercombination transition, respectively.

FIG. 3. Time-dependent emission of the Lyman-α lines of B V, C VI, and N VII: (a) absolute intensities, (b) intensities relative to the C VI emission.

FIG. 4. Spectral emission recorded with XEUS during shot 123721. Lines not normally seen in the spectrum are tentatively ascribed to the $1s^22s^22p^53s \rightarrow 1s^22s^22p^6$ and $1s^22s^22p^53d \rightarrow 1s^22s^22p^6$ transitions in neonlike Ti XIII and to $4d \rightarrow 3p$ transitions in argonlike and chlorinelike Mo XXV and Mo XXVI.

FIG. 5. Spectral emission recorded with XEUS during shot 120220. Lines are identified to orginate from iron ions and are labeled by the emitting ion.

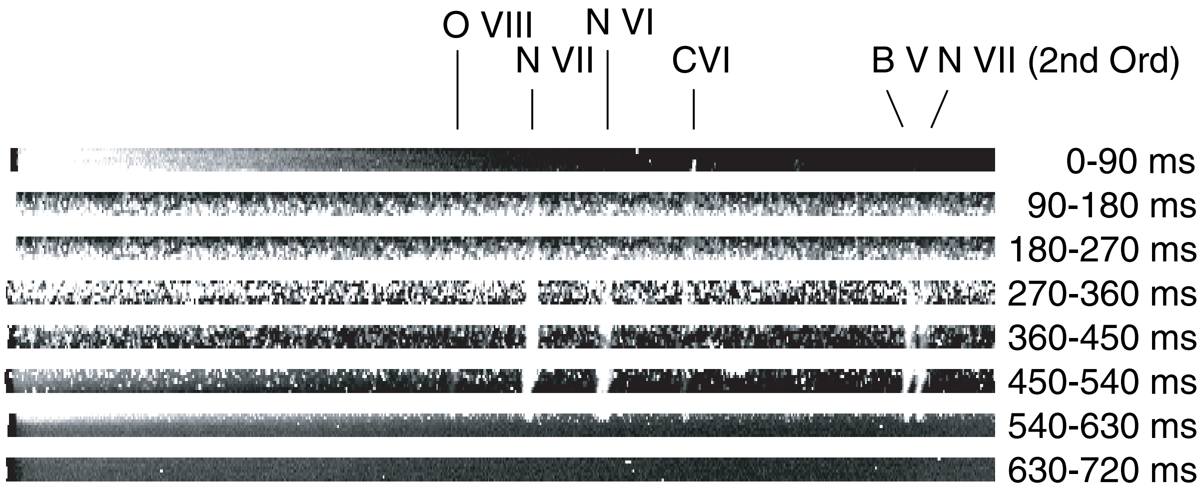
O VIII
N VII
N VI
CVI
B V N VII (2nd Ord)
0-90 ms
90-180 ms
180-270 ms
270-360 ms
360-450 ms
450-540 ms
540-630 ms
630-720 ms

Fig. 1

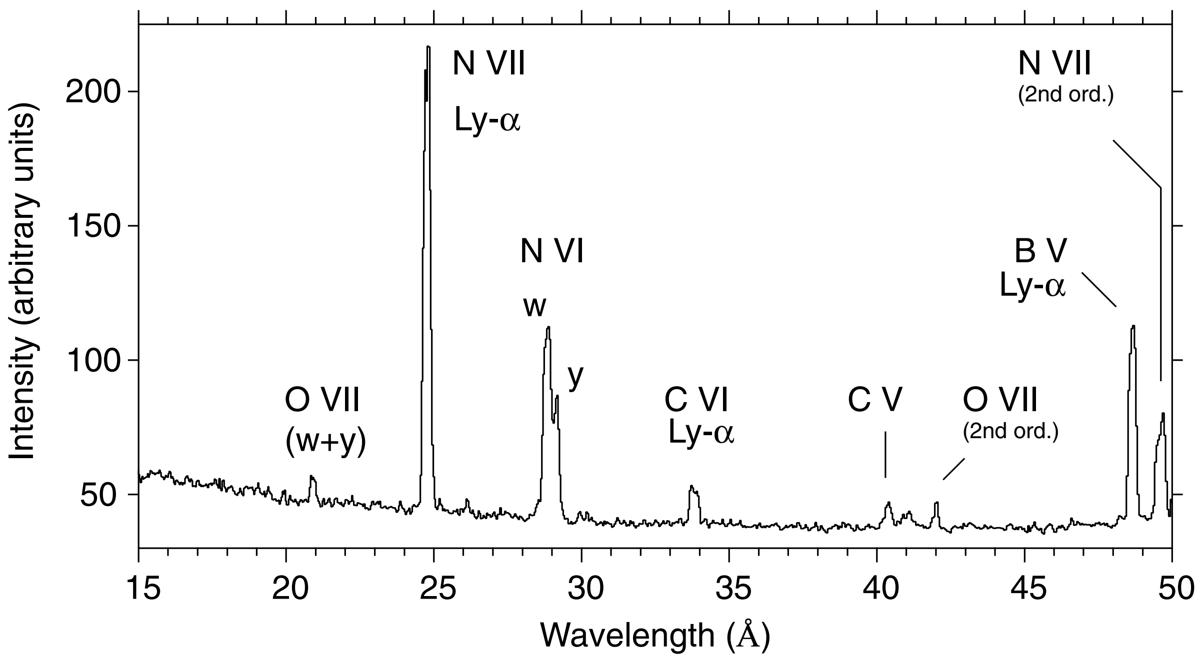

N VII
Ly-α
N VI
w
y
O VII
(w+y)
C VI
Ly-α
C V
O VII
(2nd ord.)
B V
Ly-α
N VII
(2nd ord.)
Intensity (arbitrary units)
Wavelength (Å)
200
150
100
50
15
20
25
30
35
40
45
50

Fig. 2

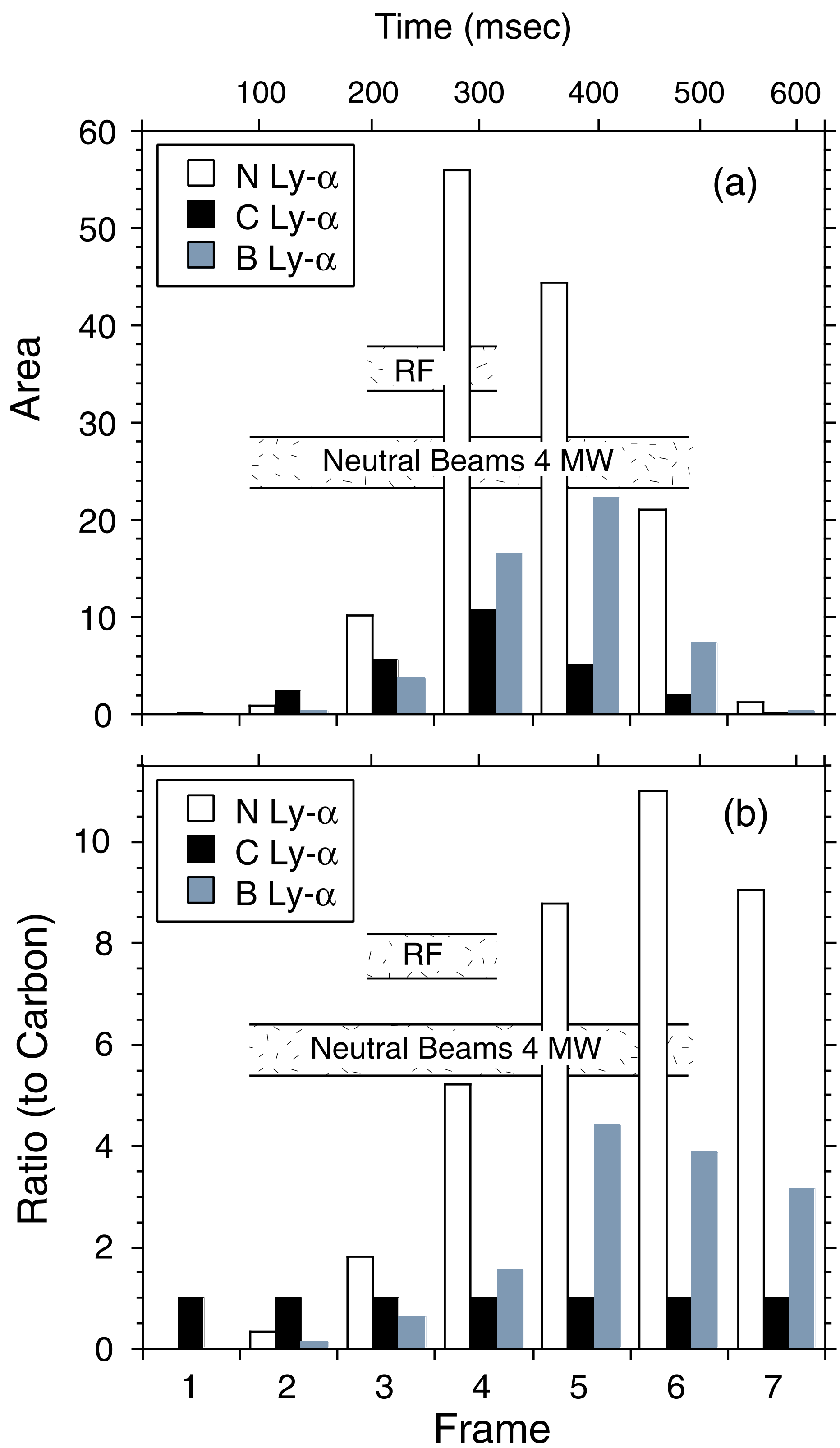
Time (msec)
100
200
300
400
500
600
60
50
40
30
20
10
0
Area
N Ly-α
C Ly-α
B Ly-α
(a)
RF
Neutral Beams 4 MW
10
8
6
4
2
0
Ratio (to Carbon)
N Ly-α
C Ly-α
B Ly-α
(b)
RF
Neutral Beams 4 MW
1
2
3
4
5
6
7
Frame

Fig. 3

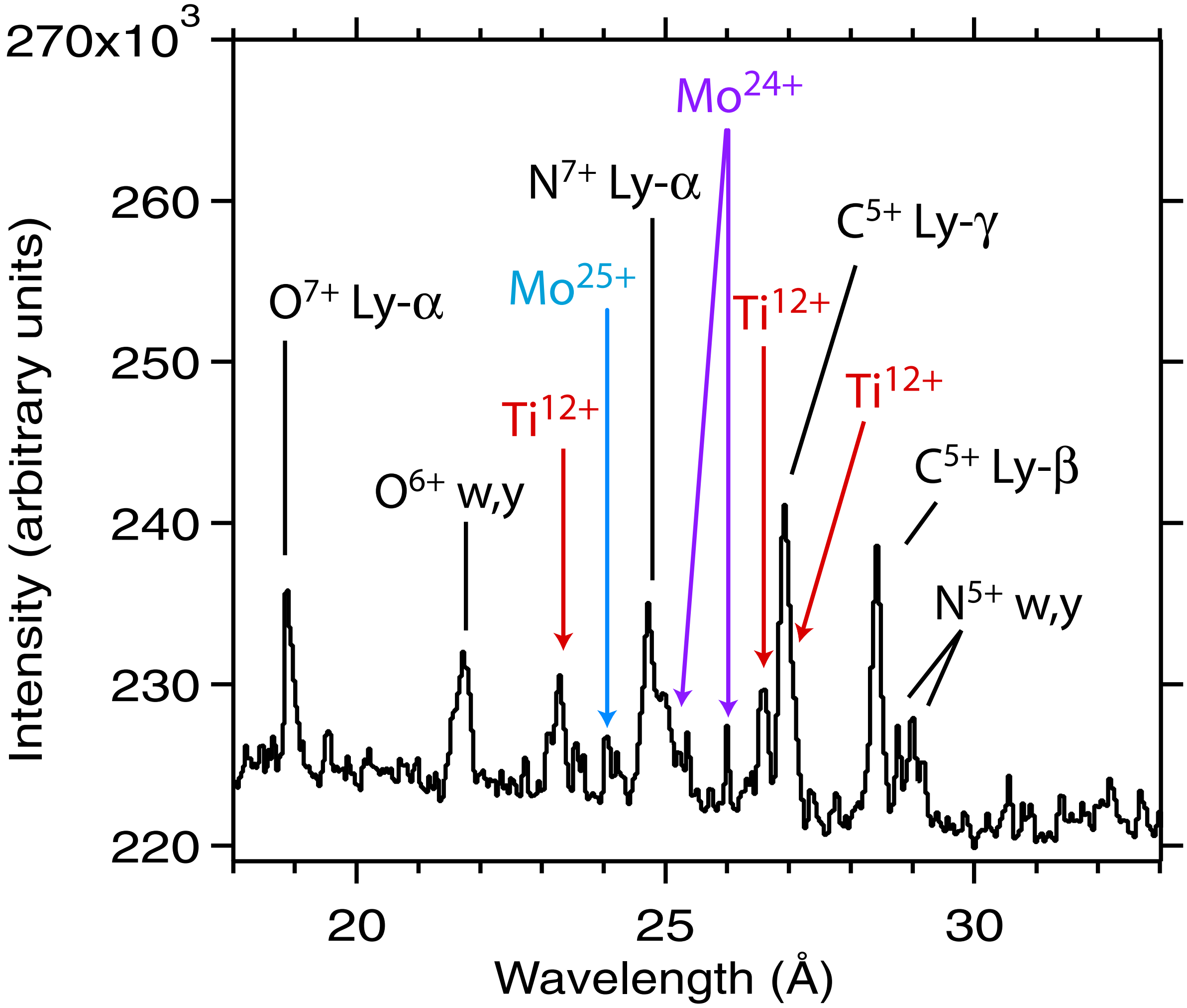
270x10^3
260
250
240
230
220
20
25
30
Wavelength (Å)
Intensity (arbitrary units)
O7+ Ly-α
O6+ w,y
Ti12+
Mo25+
N7+ Ly-α
Mo24+
Ti12+
C5+ Ly-γ
Ti12+
C5+ Ly-β
N5+ w,y

Fig. 4

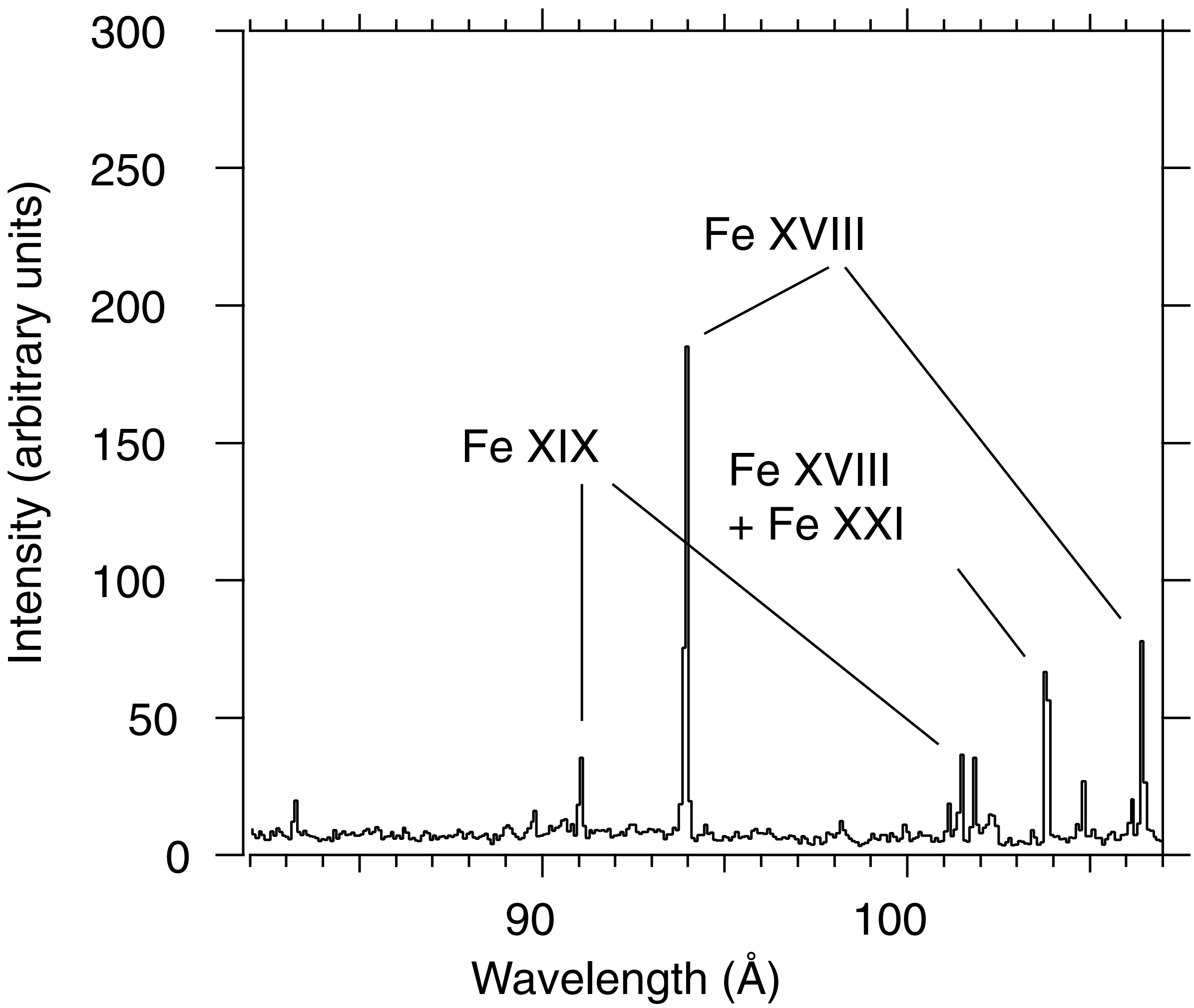

300
250
200
150
100
50
0
Intensity (arbitrary units)
90
100
Wavelength (Å)
Fe XVIII
Fe XIX
Fe XVIII
+ Fe XXI

Fig. 5